EXPERIMENTAL AND MODELING STUDIES OF CRUSH, PUNCTURE, AND PERFORATION SCENARIOS IN THE STEVEN IMPACT TEST

Kevin S. Vandersall, Steven K. Chidester, Jerry W. Forbes, Frank Garcia,
Daniel W. Greenwood, Lori L. Switzer, and Craig M. Tarver
Lawrence Livermore National Laboratory
Livermore, CA 94550

The Steven test and associated modeling has greatly increased the fundamental knowledge of practical predictions of impact safety hazards for confined and unconfined explosive charges. Building on a database of initial work, experimental and modeling studies of crush, puncture, and perforation scenarios were investigated using the Steven impact test. The descriptions of crush, puncture, and perforation arose from safety scenarios represented by projectile designs that "crush" the energetic material or either "puncture" with a pinpoint nose or "perforate" the front cover with a transportation hook. As desired, these scenarios offer different aspects of the known mechanisms that control ignition: friction, shear and strain. Studies of aged and previously damaged HMX-based high explosives included the use of embedded carbon foil and carbon resistor gauges, high-speed cameras, and blast wave gauges to determine the pressure histories, time required for an explosive reaction, and the relative violence of those reactions, respectively. Various ignition processes were modeled as the initial reaction rate expression in the Ignition and Growth reaction rate equations. Good agreement with measured threshold velocities, pressure histories, and times to reaction was calculated for LX-04 impacted by several projectile geometries using a compression dependent ignition term and an elastic-plastic model with a reasonable yield strength for impact strain rates.

INTRODUCTION

Experimental and reactive flow modeling research efforts using the Steven Impact Test at Lawrence Livermore National Laboratory[1-5] and a modified version of this test at Los Alamos National Laboratory[6-8] have greatly increased the fundamental knowledge and practical predictions of impact safety hazards for confined and unconfined explosive charges. The dominant microscopic mechanisms that control the initial ignition during compaction of a small volume of the explosive charge have been identified as friction, shear, and strain. However, the relative importance of these three processes in each ignition scenario has not yet been determined experimentally. While attempting to simulate possible accident scenarios, five different projectile geometries have been used to vary the initial impact pressure and pulse time duration on pristine, aged, and previously damaged HMX-based high explosives. Embedded carbon foil and carbon resistor gauges have been used to determine the pressure histories at various locations in the explosive charges. High-speed cameras and blast wave gauges have been used to measure the time required for an explosive reaction and the relative violence of those

reactions, respectively. All of this data has been used to develop a predictive impact ignition reactive flow model based on the Ignition and Growth model for shock initiation and detonation.

In an effort to determine the relative importance of friction and shear in impact ignition and test three ignition scenarios; crush, puncture, and perforation, the Steven test projectiles and the explosive targets were modified. To study crush, the previously used flat projectile impacted unconfined or very weakly confined explosive charges. For the puncture scenario, a long sharp "nose" was added to the usual curved projectile so that the steel cover plate and the entire explosive charge is penetrated by this "nose." Threshold velocities, pressure histories, times to reaction, and violence of reaction was measured for several HMX-based explosives: LX-04 (85% HMX, 15% Viton-A), PBX 9501 (95% HMX, 2.5% Estane, 2.5% BDNPA-F), LX-10 (95% HMX, 5% Viton-A), LX-14 (95.5% HMX, 4.5% Estane 5702-F1), and PBX 9404 (94% HMX, 3% NC, 3% CEF). In the case of perforation, one practical issue that arose was the safety of explosives in a transportation scenario where the transportation hooks that retain the apparatus could become dislodged and act as projectiles into the assembly. As a very direct approach, a transportation hook was used as a projectile into a Steven test target that would "perforate" the cover.

Initial reactive flow model predictions of impact pressure and pulse duration for five HMX-based explosives were based on a simple elastic-plastic material model plus the Jones-Wilkins-Lee (JWL) equation of state for the unreacted explosive based on shock compression experimental data.[2-4] This agreement with embedded gauge records was improved by using a material model for the unreacted explosive that was extended to include much more detail of the compression process at pressures below 60 MPa, especially just above and just below the effective yield strength of the solid explosive at relatively high strain rates.[5] In this paper, an Ignition and Growth reactive flow model for LX-04 calibrated to the threshold velocities for three previously used projectiles is used to predict measured threshold velocities for the crush and puncture scenarios.

EXPERIMENTAL GEOMETRY

The experimental geometry of the Steven impact test target and five projectiles are shown in Figure 1. The 5 projectiles consist of 4 different steel cylinders with impact surfaces of different spherical radii; 3.175, 30.05, 6.356, and 203.2 mm, respectively, and a transportation hook screwed into a steel cylinder. Projectiles #2-5 (1.6 kg) weigh more than Projectile #1 (1.2 kg), to test projectile mass intermediates between projectile #1 and the 2 kg mass used by Idar et. al.[6] A gas gun accelerates a test projectile into a 110 mm diameter by 12.85 mm thick explosive charge confined by a 3.18 mm thick steel plate on the impact face, a 19.05 mm thick steel plate on the rear surface, and 26.7 mm thick steel side confinement. A later version of the target replaced the 26.7 mm steel side confinement with a PMMA surround ring to allow the light generated from the reaction to be observed by a high-speed camera. It also serves as a low-density medium for resolution by x-ray imaging. The explosive charge is press fit into a Teflon retaining ring, thus eliminating air gaps and insuring full confinement.

For these experiments, 76 mm and 101 mm diameter smooth bore gas guns were both utilized, the latter being used so as the hook projectile would adequately fit inside the bore. An additional note is that the 76 mm diameter gun fires onto an outdoor firing table, while the 101 mm gun fires into a large capsule shaped stainless steel firing tank. In the 76 mm diameter gun, the steel projectile heads (see Figure 1) are attached to an aluminum sabot body that is accelerated via compressed helium gas into the target. The 101 mm diameter experiments were carried out using the hook screwed into the 6.01 cm diameter steel body and attached to a polycarbonate sabot. A primer charge of 20 g H870 primer powder was used to accelerate the entire projectile assembly with plates of various materials and thickness attached to the back of the sabot to vary the total mass, which allowed different projectile velocities to be generated.

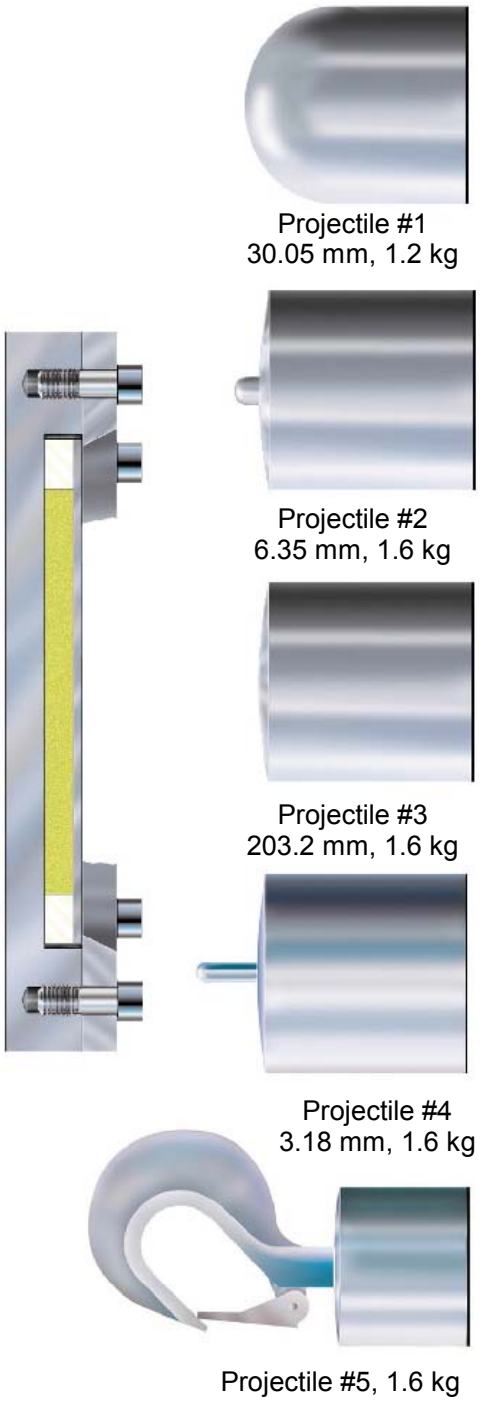

FIGURE 1. SCHEMATIC OF THE STEVEN TEST ARRANGEMENT SHOWING THE 5 DIFFERENT PROJECTILE STYLES AND 1ST VERSION OF THE TARGET DESIGN. NOTE HOOK PROJECTILE IS NOT TO SCALE WHEN COMPARED TO OTHERS.

In most cases, 4 external blast overpressure gauges were placed around the target for direct comparison to the Susan test data[9]. Placement was 3.05 meters away in the 76 mm gun experiments and 1.53 meters away in the 101 mm diameter gun arrangement. Although the placement of the gauges for the 101 mm diameter gun was desired to be 3.05 meters, the 3.66 meter tank diameter did not permit the placement at this distance.

EXPERIMENTAL RESULTS

A. Target Design Testing

The target fixture materials were changed for using x-ray diagnostics and the new target assembly was tested on the 76 mm gun to determine the effect of the change on the HE's threshold impact velocity. Both targets were tested at similar velocities and no significant difference in threshold velocity was found between the new Lucite target assembly and the original steel target assembly. A summary of the results of these tests is included in Table 1. Note that the threshold velocities are reported as the lowest velocity that achieved reaction. Therefore, the limits in parentheses are listed as plus zero and minus the difference between the experiment velocity that achieved reaction and the next lower velocity experiment that did not react.

TABLE 1. COMPARISON OF RESULTS OF ORIGINAL AND UPDATED TARGET DESIGNS. COVER PLATE WAS 1100 SERIES ALUMINUM.

TARGET DESIGN	HIGH EXPLOSIVE	THRESHOLD VELOCITY (m/s)
1 piece cup (steel)	PBX9404	18.7 (+0, -1.3)
2 piece cup (steel base with Lucite surround ring)	PBX9404	19.5 (+0, -1)

B. "Crush" Tests with Projectile #3

Although the projectile head #3 has a flat appearance, a large radius of 203 mm is actually present on the face. This is in contrast to the small radii in the projectiles #4 and 5. A previous study[4] compared the projectile #3 results to that of projectiles #1 and 2. It was found that the flatter projectiles (i.e. #3) required velocities

nearly twice as high for ignition as rounded projectiles (i.e. #1) A summary for experiments with projectile #3 to study "crush" is included in Table 2 for pristine and aged LX-04.

TABLE 2. SUMMARY OF SINGLE IMPACT TESTED THRESHOLDS FOR PROJECTILE #3.

HE TYPE	DENSITY (g/cc)	STOCK-PILE AGE (months)	THRESHOLD VELOCITY (m/s)
LX-04	1.870	0	61.5 (+0, -0.8)
LX-04	1.867	256	61.9 (+0, -1.2)

C. "Puncture" Tests with Projectile #4

A total of 5 shots at various velocities (25.7, 25.3, 25.3, 37.5, and 44.8 m/s) were performed with projectile #4 and the original steel cover plate. The tip bent during impact on all 5 shots and did not puncture the steel cover plate. Therefore an aluminum cover plate was used. To determine the effects of changing the cover plate material, a series of experiments was performed using aluminum cover plates. A summary of the results from these experiments is outlined in Table 3.

TABLE 3. SUMMAEY OF RESULTS FROM "PUNCTURE" TESTS.

EXPT DETAIL	HE TYPE	THRESHOLD VELOCITY (m/s)
Projectile #4, Al Cover Plate	PBX9404	18.7 (+0, -1.3)
Projectile #4, Al Cover Plate	PBX9501	22.8 (+0, -0.9)
Projectile #4, Al Cover Plate	LX-04	22.6 (+0, -0.6)

Tests were also performed with projectile #2 impacting bare HE. Although only 2 tests were performed, one at 18.3 and the other at 19.2 m/s, both impacted PBX9404 sample discs and only a small hole was present in the recovered and unreacted PBX9404 sample discs.

D. "Perforation" Tests with Projectile #5

A summary of the hook projectile experiments performed in the 101 mm gun is shown in Table 4. The details include the experiment number, velocity achieved, total projectile mass, the projectile type, whether reaction occurred, and comments. It can be seen that experiments WRL183 and 185 did not react at velocities of 37 and 67 m/s, respectively. Conversely, reaction was observed in experiments WRL184 at 69 m/s and WRL186 at 72 m/s. The recovery of components after the experiment reveals (see comments in Table 3) that perforation and tearing of the front cover by the hook is observed as the threshold for reaction is approached and exceeded.

A display of high speed camera images can be seen in Figure 2 with a frame reference number to the left and a relative time at the lower center. The projectile can be seen in frame 1, at time t_1 in flight and approximately at time of impact, t_2 (t_1 +568 μs), in frame 2. Later time in frames 3,4, and 5 reveals the various stages of reaction observed from the first bit of light generated in frame 3 (t_2 + 142 μs) to the reaction debris starting to be expelled to the target in frame 5 (t_2 + 426 μs). The exposure for the camera was set to 10 μs and the interframe time was 142 μs. From this experimental high-speed camera evidence, reaction goes from initiation to considerable reaction product expulsion in approximately 400-500 μs. This basic qualitative observation supports that the violence would be below that of a high order detonation.

TABLE 4. SUMMARY OF THE HOOK PROJECTILE IMPACTING PBX 9404 TARGETS.

EXPT	VELOCITY	TOTAL PROJECTILE MASS (KG)	PROJECTILE TYPE	REACTION?	COMMENTS
WRL183	37 m/s	3	HOOK	NO	Target cover dented
WRL183A	71 m/s	2.2	FLAT	YES	2nd impact of WRL183
WRL184	69 m/s	2.4	HOOK	YES	Tear from hook in cover
WRL185	67 m/s	2.7	HOOK	NO	Broke apart, tear in cover
WRL186	72 m/s	2.5	HOOK	YES	Tear from hook in cover

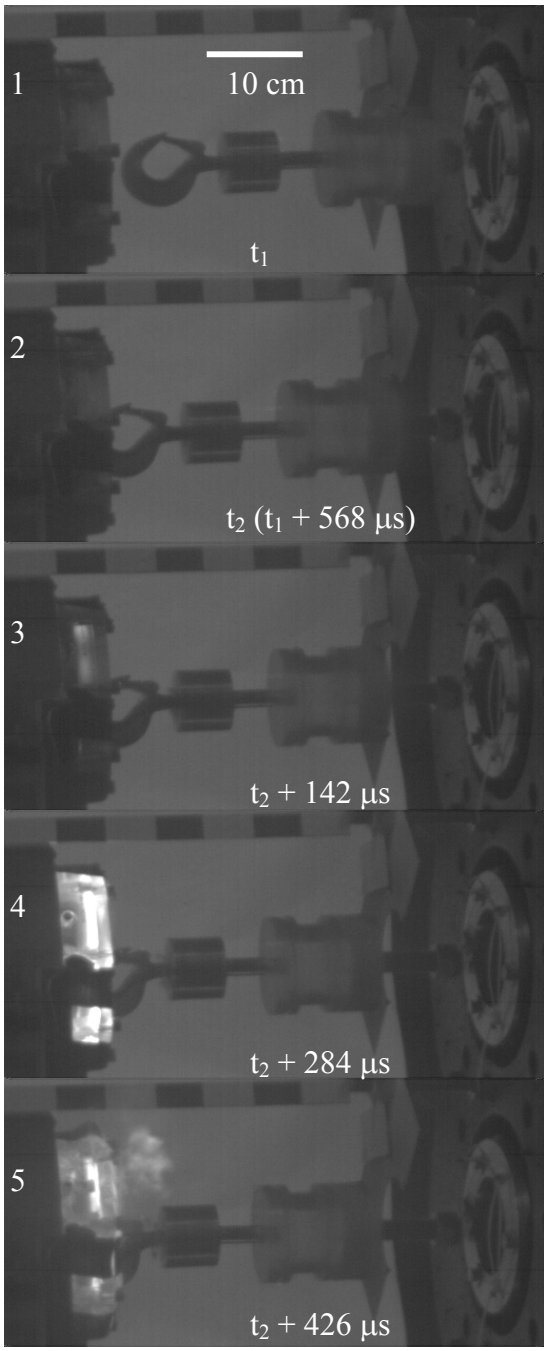

FIGURE 2. SEGMENT OF HIGH-SPEED CAMERA FRAMS SHOWING THE IMPACT OF HOOK PROJECTILE INTO THE STEVEN TEST TARGET FOR EXPERIMENT WRL184. THE CAMERA TOOK FRAMES AT INTERVALS OF 142 μS AND EXPOSURE TIME OF 10 μS.

IGNITION & GROWTH REACTIVE FLOW MODELING RESULTS

The ignition thresholds for HMX-based explosive reactions under the pressure - time duration conditions created by the five different Steven Test projectiles provide a difficult test for reactive flow modeling. All 5 different impact geometries are being modeled using the Ignition & Growth reactive model in the hydrodynamic computer codes DYNA2D, CALE, LS-DYNA[10], and ALE3D. The ignition of the explosive during impact is more difficult to model than that produced by strong shock and detonation waves, because, during impact, several mechanisms (friction, shear, strain, etc.) are occurring at relatively low pressures where the explosive acts as an elastic-plastic material. The initial amount of explosive reacted is approximately 0.1% followed by compression states that last several hundred microseconds. At the higher pressures and compression rates of shock initiation and detonation, the explosive deforms plastically, and "hot spots" are created that react a percentage of the explosive approximately equal to the initial void volume in less than one microsecond. The exact "hot spot" formation mechanisms are not as important because many relatively large, heated regions are rapidly created. Thus, in impact ignition modeling, more attention has to be paid to the elastic-plastic properties and the various ignition mechanisms that cause the first 0.1 – 1.0% of the HMX particles to react.

Many ignition mechanisms have been modeled as the first reaction term in the impact Ignition & Growth model (friction, shear, strain rate, Browning's formula,[8] etc.). All of these mathematical forms can be made to ignite the needed amount of material, but no experimental evidence of the dominance of one ignition mechanism for a certain projectile or pressure range has yet to be obtained. Therefore, a compression dependent ignition rate using current relative density to the fourth power, which is equivalent to pressure squared at these pressures, is used here.

The first step in understanding the Steven impact test was to model Projectile #1 (Tantalum at that time) in DYNA2D to determine the material deformation response and to develop a

frictional work criteria that could be used for analytical predictions.[1] Then the Ignition & Growth reactive flow model for shock initiation and detonation was adapted to the much lower pressures and longer time durations observed in the Steven Test. Initially, this model was used to determine the conditions under which reactions would occur in several hundred microseconds.[2] As more velocity threshold data for several pristine and damaged HMX-based explosives became available, Ignition & Growth parameters were derived using a compression dependent ignition term similar to the frictional work or $p^2\tau$ critical energy criterion so that practical impact problems could be predicted for the first time.[3,4]

After embedded pressure gauges were added to the Steven Test instrumentation, measured pressure histories could be modeled and more realistic descriptions of the unreacted explosive could be formulated.[5] The Jones-Wilkins-Lee (JWL) equations of state from shock initiation studies were found to predict higher impact pressures than those measured by embedded pressure gauges. Improved elastic-plastic models yielded lower impact pressures.[5] The most important factor was the use of lower yield strengths for the unreacted explosive at the lower strain rates occurring during impact as compared to the effective yield strengths for shock compression. With this improved description of the solid, velocity thresholds for reaction and the times to reaction were calculated for PBX 9501 impacted by Projectile #1.[5]

In this paper, the Ignition & Growth model is applied to the effect of different projectile geometries on reaction thresholds. Unfortunately, threshold projectile velocities for reaction in all 5 HMX-based explosives (PBX 9404, PBX 9501, LX-10, LX-04, and LX-14) have not yet been determined for all 5 projectile types. Only LX-04 has been studied using the multiple Projectile types # 1, 2, and 3. The threshold velocities for LX-04 are 45(+0, -5.0), 30.7 (+0, -0.9), and 61.9 (+0, -1.2) m/s for Projectiles # 1, 2 and 3, respectively. The calculated time that the projectile keeps the target under compression for these projectiles are approximately 400 μs, 700 μs, and 280 μs, respectively. The maximum pressure pulses (approximately 0.1 GPa for 60 – 80 μs) are much shorter than these rebound times, but reaction can continue to grow as long as the pressure and compression remain positive in the explosive charge.

Using the usual JWL unreacted equation of state for LX-04 with an experimentally measured shear modulus of 3.52 GPa and a yield strength of 0.065 GPa for impact-type strain rates, the Ignition & Growth model yielded threshold velocities of 43 (+0, -1.0), 32 (+0, -1.0), 61 (+0, -2.0) m/s, respectively. The calculated times to reaction and pressure histories were close to experimental framing camera and embedded gauge records, respectively. Table 4 lists the Ignition & Growth parameters used for LX-04 to obtain this agreement with threshold velocities for reaction measured with 3 different projectiles. This type of predictive modeling will be attempted on the other explosives when the experimental data becomes available.

TABLE 4. IMPACT IGNITION & GROWTH PARAMETERS FOR LX-04, ρ_0=1.865 g/cm^3.

UNREACTED JWL	PRODUCT JWL
A=7320 Mbar	A=13.3239 Mbar
B=-0.052654 Mbar	B=0.740218 Mbar
R_1=14.1	R_1=5.9
R_2=1.41	R_2=2.1
ω=0.8867	ω=0.450
C_V=2.7806x10^{-5} Mbar/K	C_V=1.0x10^{-5} Mbar/K
T_o = 298ºK	E_o=0.095 Mbar
Shear Modulus=0.0352 Mbar	-
Yield Strength=0.00065 Mbar	-
REACTION RATES	
a=0	x=4.0
b=0.667	y=1.0
c=2.0	z=2.0
d=2.0	F_{igmax}=0.01
e=0.333	F_{G1max}=1.0
g=1.0	F_{G2min} =0.01
I=1000 μs^{-1}	G_1=130 Mbar^{-2}μs^{-1}
-	G_2=400 Mbar^{-1}μs^{-1}

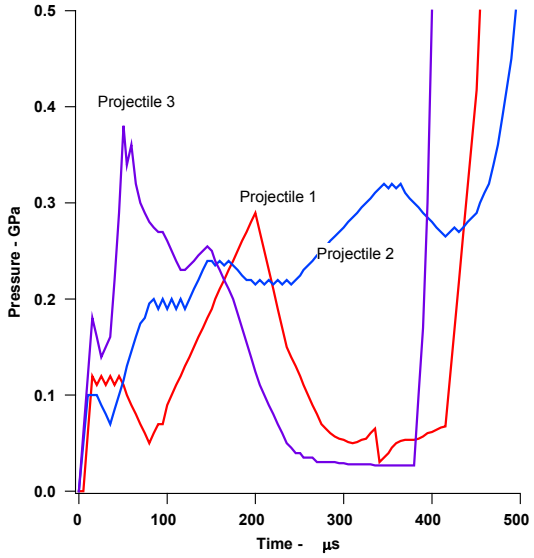

FIGURE 8. PRESSURE HISTORIES FOR LX-04 IMPACTED BY PROJECTILES 1, 2, AND 3 AT THE MINIMUM VELOCITIES THAT CAUSE OBSERVABLE REACTION.

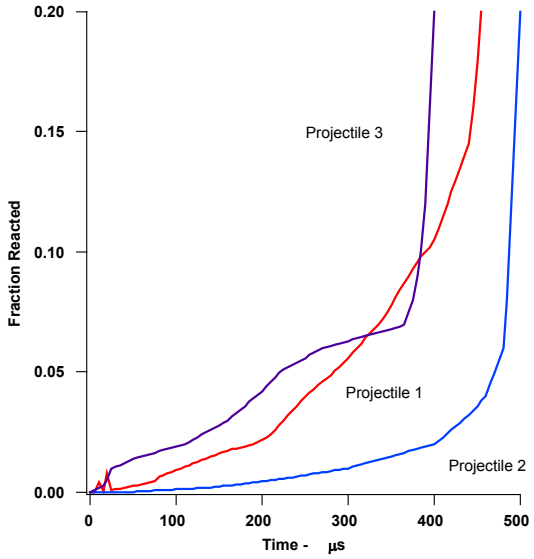

FIGURE 9. FRACTION REACTED HISTORIES FOR LX-04 IMPACTED BY PROJECTILES 1,2, AND 3 AT THE MINIMUM VELOCITIES THAT CAUSE OBSERVABLE REACTION.

The LX-04 model calibrated to three threshold velocities for Projectiles #1, #2, and #3 was then applied to predicting the measured threshold velocities for puncture scenario (Projectile #4). Figure 8 shows pressure histories for LX-04 impacted by the projectiles #1,2, and 3 at the minimum velocities that cause observable reaction. As a companion to this plot, Figure 9 displays the fraction reacted histories for LX-04 impacted by projectiles #1,2, and 3, also at the minimum velocities that cause reaction. The predicted threshold velocity for LX-04 with an aluminum cover plate impacted by the puncture probe is 24 (+0, -2) m/s, which agrees well with the experimental value of 22.3 (+0, -0.6) m/s. The input pressures and pulse time durations for Projectile #4 are similar to the other three projectiles so the LX-04 reactive flow model was not extended far from regions of pressure and time for which it was calibrated. However, the material models used to model penetration of the aluminum plate were far too simple and must be improved before realistic predictive modeling can be done. More experiments with Projectile #4 on the other explosives using embedded pressure gauges are required.

Modeling Projectile #5 (the hook) is an even greater challenge that is still being addressed. The hook is truly a three-dimensional object that can not be well represented in two-dimensional codes. The complete 3D Steven Test geometry is being run in LS-DYNA and ALE3D. Since the hook is much less thick than the other projectiles, its pulse duration is much less than those of the other Steven Test projectiles. Thus its threshold velocity for PBX 9404 (69 m/s) is much higher than that of Projectile #1 (32 m/s). This is analogous to short shock pulse durations requiring higher pressures for shock initiation in solid explosives.[11] The frictional work criteria has been successful in predicting a threshold for the hook projectile. Thus far, the 3D modeling with reactive flow has produced realistic impact pressures and time durations for the PBX 9404 hook experiments, however, the correct ignition term that will calculate the hook reaction thresholds while still reproducing the other 4 projectile thresholds has not yet been determined. Additional experimental data for the hook projectile #5 on the other explosives is required.

DISCUSSION

Embedded gauge records implied that puncture and crush ignitions occur under similar but slightly lower stresses than those measured for previous scenarios. The measured times to explosive reaction were similar to previous scenarios for crush (several hundred microseconds) but shorter (tens of microseconds) for puncture environments. The threshold velocity (impact sensitivity) for the hook projectile was found to be 69 (+0, -2) m/s impacting PBX9404. The measured violence of reaction for the crush, puncture and perforation conditions were similar to those previously measured (i.e. much less violent than an intentionally produced detonation in a Steven Test charge). For studies on "perforation," only high-speed photography and blast wave data is available to date and gauged experiments are forthcoming.

The LX-04 Ignition and Growth reactive flow model calibrated to the threshold velocities for the three previously used projectiles accurately predicted the measured threshold velocities for the crush and puncture scenarios. This was done by improving the material model used for the unreacted LX-04 explosive by including much more detail of the compression process at pressures below 65 MPa, especially just above and just below the effective yield strength of the solid explosive at relatively high strain rates. This improved material model/equation of state description of the unreacted explosive also produced better agreement with embedded pressure gauge records.

SUMMARY AND FUTURE WORK

A new target design was incorporated that replaces the one-piece steel cup with a steel backing with a Lucite (PMMA) ring was used and no significant difference in threshold velocity was found. The threshold (impact sensitivity) for the hook projectile was found to be 69 (+0, -2) m/s impacting PBX9404.

Gauged experiments with the hook projectile impacting PBX9404 and the other explosives are needed and currently in progress.

ACKNOWLEDGEMENTS

The 76 mm gun grew; Karen Luis, Don Gonzalez, John Elliott, Art Caya, John Given, and Bruce Greenfield at Site 300 (Bunker 812) are acknowledged for their hard work. The 101 mm gun crew; Ernie Urquidez, Brian Cracciola, and Gary Steinhour are also thanked for their outstanding efforts. This work was performed under the auspices of the U. S. Department of Energy by the University of California, Lawrence Livermore National Laboratory under Contract No. W-7405-Eng-48.

REFERENCES

1. Chidester, S.K., Green, L.G., and Lee, C.G., "A Frictional Work Predictive Method for the Initiation of Solid High Explosives from Low Pressure Impacts," Tenth International Detonation Symposium, ONR 33395-12, Boston, MA 1993, pp. 785-792.
2. Chidester, S. K., Tarver, C. M., and Lee, C. G., "Impact Ignition of New and Aged Solid Explosives," Shock Compression of Condensed Matter-1997, edited by S.C. Schmidt et. al., AIP Conference Proceedings 429, AIP Press, New York, 1998, pp. 707-710.
3. Chidester, Steven K., Tarver, Craig M., and Garza, Raul, " Low Amplitude Impact Testing and Analysis of Pristine and Aged Solid High Explosives," Eleventh (International) Symposium on Detonation, ONR 33300-5, Arlington, VA, 1998, pp. 93-100.
4. Chidester, S. K., Tarver, C. M., DePiero, A. H., and Garza, R. G., "Single and Multiple Impact of New and Aged High Explosives in the Steven Impact Test," Shock Compression of Condensed Matter-1999, M.D. Furnish, L. C. Chhabildas, and R. S. Hixson, eds., AIP Conference Proceedings 505, New York, 2000, P. 663-666.
5. Niles, A. M., Garcia, F., Greenwood, D. W., Forbes, J. W., Tarver, C. M., Chidester, S. K., Garza, R. G., and Switzer, L. L., "Measurement of Low Level Explosives Reaction in Gauged Multi-dimensional Steven Impact Tests," Shock Compression of Condensed Matter-2001, Furnish, M. D., Thadhani, N. N., and Horie, Y, eds. CP-620, AIP Press, New York, (2002).

6. Idar, D. J., Lucht, R. A., Straight, J. W., Scammon, R. J., Browning, R. V., Middleditch J., Dienes, J. K., Skidmore, C. B., and Buntain, G. A., Eleventh International Detonation Symposium, Aspen, CO, 1998, pp. 101-110.
7. Scammon, R. J., Browning, R. V., Middleditch, J., Dienes, J. K. Haverman, K. S., and Bennett, J. G., Eleventh International Detonation Symposium, Aspen, CO, 1998, pp. 111-118.
8. Browning, R. V., in Shock Compression of Condensed Matter-1995, S. C. Schmidt and W. C. Tao, eds, AIP Press, New York, 1996, p. 405-408.
9. Dobratz, B.M. and Crawford, P.C., LLNL Explosives Handbook, Lawrence Livermore National Laboratory Report UCRL-52997 change 2, 1985.
10. LS-DYNA Keyword User's Manual, Version 960, Livermore Software Technology Corporation, March 2001.
11. Tarver, C. M., Hallquist, J. O., and Erickson, L. M., Eighth Symposium (International) on Detonation, Naval Surface Weapons Center NSWC 86-194, Albuquerque, NM, 1985, p. 951.